



Article

# Remodeling Membrane Binding by Mono-Ubiquitylation

Neta Tanner<sup>1</sup>, Oded Kleinfeld<sup>2</sup>, Iftach Nachman<sup>1</sup> and Gali Prag<sup>1,3,\*</sup>

<sup>1</sup> School of Neurobiology, Biochemistry and Biophysics, The George S. Wise Faculty of Life Sciences, Tel Aviv University, Tel Aviv 69978, Israel

<sup>2</sup> Faculty of Biology, Technion—Israel Institute of Technology, Haifa 32000, Israel

<sup>3</sup> Sagol School of Neuroscience, Tel Aviv University, Tel Aviv 69978, Israel

\* Correspondence: prag@tauex.tau.ac.il; Tel.: +972-364-09-828

Received: 16 June 2019; Accepted: 29 July 2019; Published: 31 July 2019



**Abstract:** Ubiquitin (Ub) receptors respond to ubiquitylation signals. They bind ubiquitylated substrates and exert their activity *in situ*. Intriguingly, Ub receptors themselves undergo rapid ubiquitylation and deubiquitylation. Here we asked what is the function of ubiquitylation of Ub receptors? We focused on yeast epsin, a Ub receptor that decodes the ubiquitylation signal of plasma membrane proteins into an endocytosis response. Using mass spectrometry, we identified lysine-3 as the major ubiquitylation site in the epsin plasma membrane binding domain. By projecting this ubiquitylation site onto our crystal structure, we hypothesized that this modification would compete with phosphatidylinositol-4,5-bisphosphate (PIP<sub>2</sub>) binding and dissociate epsin from the membrane. Using an *E. coli*-based expression of an authentic ubiquitylation apparatus, we purified ubiquitylated epsin. We demonstrated *in vitro* that in contrast to *apo* epsin, the ubiquitylated epsin does not bind to either immobilized PIPs or PIP<sub>2</sub>-enriched liposomes. To test this hypothesis *in vivo*, we mimicked ubiquitylation by the fusion of Ub at the ubiquitylation site. Live cell imaging demonstrated that the mimicked ubiquitylated epsin dissociates from the membrane. Our findings suggest that ubiquitylation of the Ub receptors dissociates them from their products to allow binding to a new ubiquitylated substrates, consequently promoting cyclic activity of the Ub receptors.

**Keywords:** ubiquitylation; Ub receptor; phosphatidylinositol phosphate

## 1. Introduction

Ubiquitylation regulates most cellular pathways in eukaryotes [1]. Ubiquitin (Ub) signals are written and edited by a multiplexed network of E1 (Ub-activating enzyme), E2 (Ub-conjugating enzyme), E3 (Ub-ligase), and deubiquitylating enzymes in a tightly regulated manner. Intriguingly, the same Ub molecules code many different cellular outcomes [2]. How do cells correctly interpret these Ub codes? It has become evident that hundreds of Ub receptors read and respond to Ub signals by tethering Ub binding domains (UBDs) to a “response element”. Moreover, Ub receptors possess modules that sense the cellular context (hereafter “context domain”), which allows them to function in an appropriate spatiotemporal manner. Enigmatically, Ub receptors are themselves regulated by ubiquitylation [3–5]. For example, in two independent studies, both Bonifacio and our own laboratory demonstrated that ubiquitylation promotes the dissociation of the Ub receptors Rabex5 and Vps9 (a human and its yeast orthologue, respectively) from their ubiquitylated cargos [6,7]. The UBDs of these Ub receptors are tethered to a GEF (guanine nucleotide exchanging factor) domain. They bind *in trans* their ubiquitylated targets on Rab5 endosomes to synchronize GEF activity with ubiquitylated cargo trafficking. Following ubiquitylation of these Ub receptors, their UBDs leave the Ub moiety on the cargo and bind the self-conjugated Ub *in cis*. It was suggested that deubiquitylation then takes place

to enable the cyclic activity of these Ub receptors. Similarly, the Ub receptor Rpn10 functions as a shuttling receptor that catches the ubiquitylated targets and transports them for degradation at the proteasome. We have demonstrated that following the ubiquitylation of Rpn10 on the proteasome, its conjugated Ub clashes with Rpn9, and consequently the ubiquitylated Rpn10 dissociates from the proteasome [8]. It has been suggested that the dissociation of ubiquitylated Rpn10 followed by deubiquitylation allows the recurrent shuttling of Rpn10 with its ubiquitylated cargo to the proteasome. The above two marginally different mechanisms are both conducive to the cyclic activity of these particular Ub receptors.

Here, we asked whether the activity of epsin, a Ub receptor that functions at the plasma membrane [9], might also be regulated by ubiquitylation/deubiquitylation in order to maintain its cyclic activity. Epsin proteins decode the ubiquitylation signals of the plasma membrane proteins to promote their clathrin-dependent endocytosis [10–12]. In epsin, a tandem of UBDs [comprising ENTH (Epsin N-Terminal Homology domain) and two UIMs (Ub-Interacting Motif)] is linked to the response elements that recruit the endocytic machinery (Figure 1). As epsin ambushes its ubiquitylated targets at the plasma membrane, its context domain (ENTH) specifically associates with the membrane lipid phosphatidylinositol-4,5-bisphosphate (PIP<sub>2</sub>) [9,13]. An elegant study by McMahon and co-workers demonstrated that the amphipathic N-terminal  $\alpha$ -helix (hereafter, H<sub>0</sub>) of rat epsin directly interacts with PIP<sub>2</sub> and induces membrane curvature for the downstream formation of clathrin-coated pits [9]. Kozlov and co-workers calculated and demonstrated that H<sub>0</sub> not only induces membrane curvature, but also contributes to membrane fission at the end of the endocytosis [14,15]. The emerging vesicles fused with early endosomes, resulting in the translocation of both the ubiquitylated cargo and epsin to early endosomes. As epsin functions at the plasma membrane, we postulated that a retrograde mechanism dissociates epsin from the early endosomes to enable cyclic functioning. Based on our studies with the Ub receptors Vps9 and Rpn10, we hypothesized that epsin ubiquitylation may also dissociate Ub–epsin from the early endosomes initiating its retrograde process. Here we describe a series of *in vitro* and *in vivo* experiments that independently tested this hypothesis.

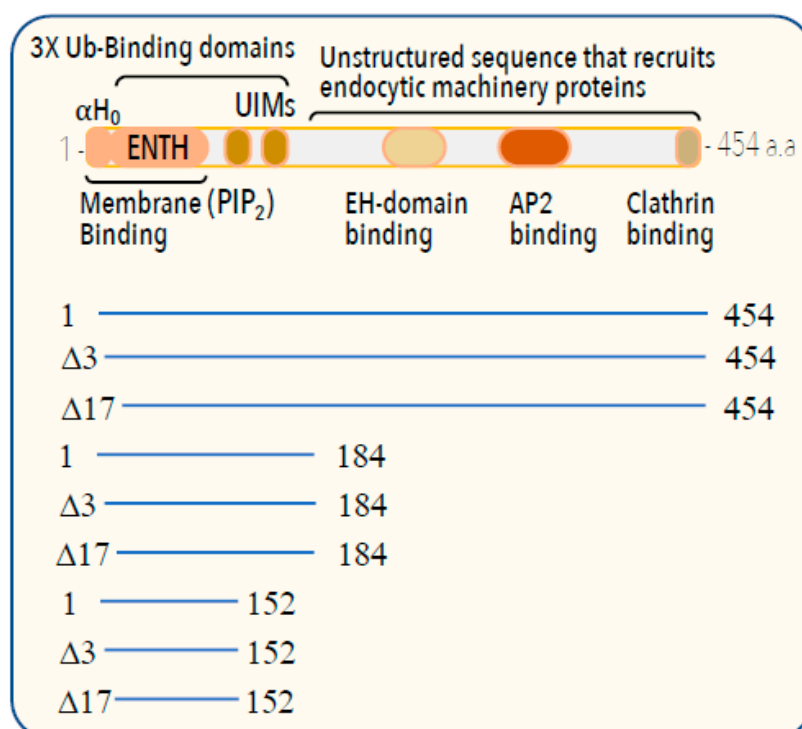


**Figure 1.** Domain architecture of epsin. The domains of yeast Ent1 and their main functions and partners are shown. Below, the main constructs examined in this study are shown.

## 2. Materials and Methods

### 2.1. Protein Expression and Purification

To purify *apo* Ent1 Rosetta2 ( $\lambda$ DE3) BL21, *E. coli* cells were transformed with pHis<sub>6</sub>-Maltose Binding Protein (MBP)-Ent1 derivatives. For the purification of ubiquitylated Ent1, the same bacterial strain was co-transformed with pGEN and pCOG vectors to express the entire ubiquitylation cascade of Ent1, as described in [7]. The bacteria were grown in Terrific broth medium, supplemented with 50  $\mu$ g/mL streptomycin and 34  $\mu$ g/mL chloramphenicol, at 37 °C. Expression of Ent1 was induced by the addition of 0.5 mM isopropyl  $\beta$ -D-1-thiogalactopyranoside (IPTG), and the bacteria were grown for another ~20 h at 16 °C. Cells were harvested by centrifugation, and were re-suspended in lysozyme buffer (150 mM NaCl, 50 mM Tris-HCl pH 7.0, and 0.1 mg/mL lysozyme), supplemented with the protease inhibitor 4-(2-aminoethyl) benzenesulfonyl fluoride hydrochloride (AEBSF). A complete lysis and DNA shearing were achieved by sonication. The soluble fraction was isolated by centrifugation. The protein was purified using nickel-nitrilotriacetic acid (Ni<sup>2+</sup>-NTA) affinity chromatography, according to the manufacturer's instructions. Affinity tags were clipped by rhinovirus protease during dialysis against 150 mM NaCl and 50 mM Tris-HCl pH 7.0 buffer. Subsequently, the sample was diluted to a final concentration of 35 mM NaCl supplemented with 10% glycerol, and was loaded onto an ion exchange column (SP Sepharose fast flow, GE Healthcare) pre-equilibrated with the same buffer. The column was washed, and an NaCl gradient (35–1000 mM) was applied. The protein was eluted at ~250 mM NaCl. In the case of purification of ubiquitylated-Ent1 derivatives, an additional affinity chromatography step was added using glutathione or amylose beads, depending on the specific construct, as previously described [7]. Finally, size-exclusion chromatography (with Superdex-75 16/60 HiLoad prep-grade column) was used to further increase the protein purity and to eliminate microaggregates. The protein sample was concentrated to 10 mg/mL. Then, 100  $\mu$ L aliquots were flash-frozen in liquid nitrogen and preserved at –80 °C for downstream experiments.

### 2.2. In-Gel Digestion and Mass Spectrometry Analysis

Tryptic protein in-gel digestion was performed as described in [7,8,16]. Briefly, the proteins in each gel slice were reduced (10 mM dithiothreitol), modified with 40 mM iodoacetamide (at 25 °C), and trypsinized (modified trypsin (Promega)) at a 1:100 enzyme-to-substrate ratio for 18 h at 37 °C. The resulting tryptic peptides from each gel slice were resolved by reverse-phase chromatography on 0.075  $\times$  200 mm fused silica capillaries (Aligent Technologies J&W, Santa Clara, CA, USA) packed with Reprosil reversed-phase material (Dr Maisch GmbH, Entringe, Germany). The peptides were eluted with linear 65 min gradients of 5% to 45%, and 15 min at 95% acetonitrile with 0.1% formic acid in water, at flow rates of 0.25  $\mu$ L/min. Mass spectrometry (MS) was performed by an Orbitrap-XL mass spectrometer (Thermo) in a positive mode, using repetitive full MS scans followed by collision-induced dissociation of the seven most dominant ions selected from the first MS scan. Data analysis was performed using the Trans Proteomic Pipeline (TPP) version 4.6.3 [17]. TPP-processed centroid fragment peak lists in mzML format were searched against a database composed of *S. cerevisiae* yeast, *E. coli* proteins (Uniprot), and human Ub, supplemented with their corresponding decoy sequences. The database searches were performed using X! Tandem with the *k*-score plugin through TPP. Search parameters included trypsin cleavage specificity, with two missed cleavage sites; cysteine carbamidomethyl as a fixed modification; and lysine ubiquitylation (GG), methionine oxidation, and protein N-terminal acetylation as variable modifications. Peptide tolerance and MS/MS tolerance were set at 10 ppm and 0.8 Da, respectively. X! Tandem refinement included semi-style cleavages and variable lysine GG modification. Peptide and protein lists were generated following Peptide Prophet and Protein Prophet analysis, using a protein false discovery rate of 1%.

### 2.3. Structural Modeling

The crystal structure of Ent1–ENTH domain a.a. 17–150 (PDB 5LOZ), determined by Tanner, was the basis for our model [18,19]. We used Protein Homology/analogy Recognition Engine V 2.0 (Phyre<sup>2</sup>) to model the first 16 a.a. [20]. To obtain a complex with PI(4,5)P<sub>2</sub>, we superimposed the model with a rat Epsin1–ENTH domain complex with PI(4,5)P<sub>2</sub> [Protein Data Bank(PDB) code 1H0A]. We manually adjusted some of the amino acids at the binding pocket with Coot [21]. Finally, the structure was idealized using energy minimization with the “Idealisation” mode of Refmac5 [22]. Figures of protein/ligand structures were prepared with PyMol [23].

### 2.4. PIP<sub>2</sub>-Enriched Liposome Pull-Down Assay

A mixture of 1.5 µg of apo Ent1<sub>1–184</sub> and ubiquitylated-Ent1<sub>1–184</sub> was incubated in 20 µl of 1mM PolyPIPosomes<sup>TM</sup> (Echelon Biosciences, Catalog No.: Y-P045), and diluted in 1 mL of binding buffer containing 50 mM Tris, pH 7.5, 150 mM NaCl, and 0.05% Nonidet P-40. The blend was rotated for 10 min at room temperature and centrifuged at 30,000 rpm for 15 min. The liposome pellet was resuspended in 1 ml of binding buffer, and then centrifuged. This step was repeated three times, and the bound (pellet) and supernatant samples (at a relative ratio of 10:1) were resolved by SDS-PAGE. The hemagglutinin (HA) fusion proteins were detected by western blot analysis using anti-HA antibodies (Amersham Biosciences, Little Chalfont, UK).

### 2.5. PIP Array Binding Assay

A PIP Strip (Echelon Biosciences) binding assay was performed according to the manufacturer’s instructions. Briefly, the PIP array sheet was blocked for 1 h with a 1:1 ratio of PBS:blocking buffer (LI-COR Biosciences) at room temperature. After blocking, the PIP array was incubated for 1 h with 10 mL of 1:1 ratio of PBS:blocking buffer (LI-COR Biosciences), containing 10 µg of equal amounts of Ent1<sub>1–184</sub> and ubiquitylated-Ent1<sub>1–184</sub>. The PIP array was then washed three times and incubated with anti-His tag antibody for another hour, and then subjected to western blot analysis. The same PIP array was then incubated with anti-HA antibody for one more hour, and subjected to western blot analysis for a second detection.

### 2.6. Live Imaging of Ent1 Derivatives

*S. cerevisiae* Ent1 was PCR amplified from genomic DNA to create Ent1<sub>4–445</sub>, Ent1<sub>17–445</sub>, ENTH<sub>4–152</sub>, and ENTH<sub>17–152</sub> constructs. Ub fusion constructs were made using a PCR sewing technique, in which Ub was amplified from pGEN25 [7]. Expression vectors harboring these constructs were made by subcloning the above sequences into the pGREG600 plasmid using a homologous recombination in yeast, and isolated vectors were sequenced [24]. The vectors were transformed into yeast strain BY4741 (MAT $\alpha$  GFP::HIS3MX, ura3 $\Delta$ 0, leu2 $\Delta$ 0, his3 $\Delta$ 1, met15 $\Delta$ 0). The transformed cells were grown overnight at 30 °C in YPD (Yeast extract Peptone Dextrose media) with G418 selective medium (1% yeast extract, 2% peptone, 2% glucose, G418 200 µg/mL). Cultures were then washed, diluted, and grown for 3–4 h in inductive medium containing galactose (2%) and raffinose (1%) in the presence of G418 (200 µg/mL). The media was then discarded, and cells were resuspended in H<sub>2</sub>O. A 3–5 µL sample was put on a slide and visualized using a Nikon TiE epifluorescent microscope with an Andor Clara camera, at X100 magnification. GFP emission was imaged with 400 msec exposures.

## 3. Results

### 3.1. Yeast Ent1 Undergoes Ubiquitylation

A proteomics survey of monoubiquitylated proteins in vivo yeast had previously demonstrated that both of the epsin proteins, Ent1 and Ent2, undergo Rsp5-dependent ubiquitylation [16]. However, probably due the limited amount of ubiquitylated-Ent1, the mass spectrometry analysis in that study

could not detect the ubiquitylation sites on Ent1. In another proteomic survey in yeast, however, K103 and K148 of Ent1 and K14 of Ent2 were identified as potential ubiquitylation sites [25].

To reassess whether Ent1 undergoes mono-ubiquitylation *in vivo*, we transformed yeast cells with a plasmid that over-expresses RGS (Arg-Gly-Ser)-His<sub>8</sub>-Ub<sup>K0</sup> (in which all seven lysine residues were substituted for arginine) and extracted the ubiquitylated proteins from whole-cell lysate using rapid TCA (TriChloroacetic Acid) lysis [16]. In this experiment, we used a yeast strain that expresses an Ent1-GFP (green fluorescent protein) from its native genomic locus [26]. Proteins were enriched on an NTA column, resolved by SDS-PAGE, and subjected to western blot analysis with an anti-GFP antibody (Figure 2). A band at ~80 kDa corresponding to Ent1-GFP was clearly observed in the cell extracts that both expressed and did not express the RGS-His<sub>8</sub>-Ub<sup>K0</sup>. Moreover, only in the cells that expressed the RGS-His<sub>8</sub>-Ub<sup>K0</sup>, an additional band at ~90 kDa corresponding to ubiquitylated-Ent1 was clearly observed (Figure 2). This immunoblotting analysis suggests that the Ent1 undergoes ubiquitylation *in vivo*, and corroborates the previous data derived from the mass spectrometry survey [16].

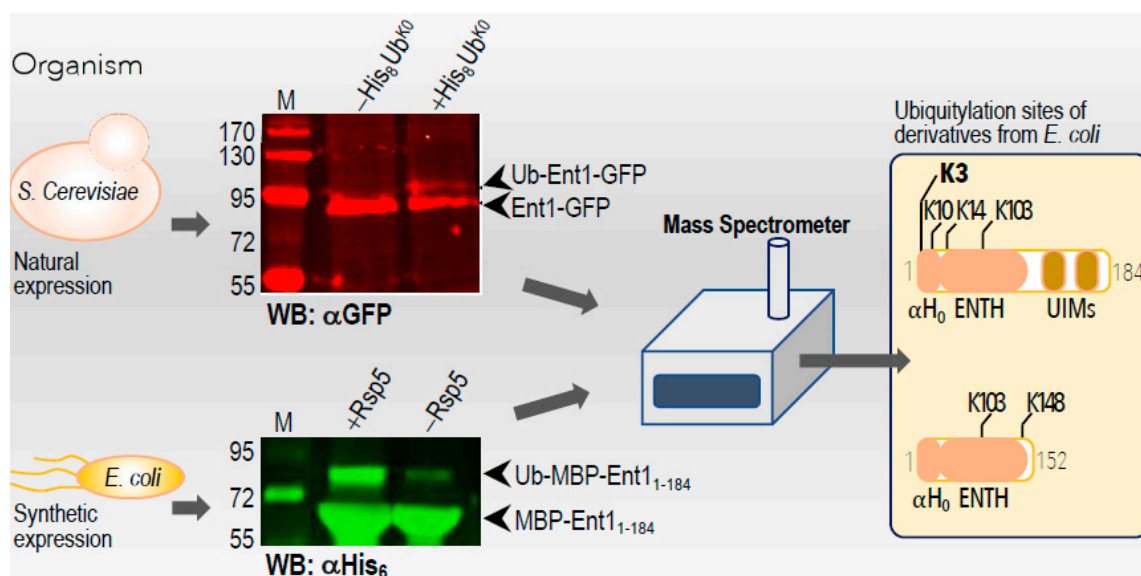


**Figure 2.** Mapping the ubiquitylation sites of Ent1. A scheme showing the approaches taken to identify the ubiquitylation sites of Ent1. *S. cerevisiae* and *E. coli* expression and purification systems described in the methods section. Purified proteins were subjected to western blot analysis with the indicated antibodies. The ubiquitylated lysine residues (Ks) identified by the mass spectrometry analysis are indicated.

### 3.2. Identification of the Ent1 Ubiquitylation Sites

To uncover the biological significance of Ent1 ubiquitylation, we sought first to identify its ubiquitylation sites. Unfortunately, the amount of RGS-His<sub>8</sub>-Ub<sup>K0</sup> ubiquitylated Ent1 derived from the yeast was again insufficient to detect the tryptic GG peptides by mass spectroscopy analysis, confirming previous results [16]. We suspect that due to the efficient deubiquitylation, the steady state amounts of modified Ent1 *in vivo* is insufficient for a mass spectrometry study. To circumvent this hurdle, we employed our *E. coli*-based synthetic biology approach to express the entire ubiquitylation apparatus of Ent1 [7]. In that system, we co-expressed His<sub>6</sub>-Ub, wheat UBA1, yeast Ubc4, yeast Rsp5, and MBP-Ent1. Using double affinity tag chromatography, we obtained milligram amounts of ubiquitylated Ent1 for downstream studies. It should be noted that we had previously demonstrated that, contrary to *in vitro* ubiquitylation assays that lead to spurious modification of several lysine residues of Rpn10 (for example [27–29]), the *E. coli*-based system faithfully recapitulates the mono-ubiquitylation on lysine 84 that is observed *in vivo* [7]. Similarly, several identified ubiquitylation sites of Rsp5 in our *E. coli*-based system were found to be identical with those found in *in vivo* studies. We performed in-gel

mass spectrometry analysis of the purified *apo* and ubiquitylated-Ent1 protein bands. Interestingly, different ubiquitylation sites were observed between Ent1 constructs that contained ENTH–UIM1 and those that contained only the ENTH domain (Ent1<sub>1-184</sub> and ENTH<sub>1-152</sub>, respectively). K3, K10, and K14, all located at the PIP<sub>2</sub> binding patch, as well as K103 of the protein that also contains the UIMs (Ent1<sub>1-184</sub>), were identified as ubiquitylation sites, with K3 being the major site that underwent the modification (Figure 2 and Supplementary Figure S1). However, in ENTH<sub>1-152</sub>, a construct that lacks the UIMs and consequently possesses only a single UBD, K103 and K148 were found to be the sole ubiquitylation sites. Based on our structures of *apo* yeast and zebrafish ENTH domains (PDB accession codes 5LOZ and 5LP0, respectively), and their homology to the human STAM1–VHS domain complex with Ub (PDB accession code 3LDZ), we constructed a structural model ENTH:Ub of non-covalent complexes [18,19]. The yeast ENTH:Ub complex provides a molecular explanation for the ubiquitylation sites found in the ENTH–UIMs construct, which better represent the natural structure of full-length Ent1 (Supplementary Figure S2). We speculate that one of the UIMs interacts non-covalently with Ub on the Rsp5 E3-ligase, “falling back” onto the ENTH domain and promoting its ubiquitylation at the lysine-rich N-terminal sequence (H<sub>0</sub>). However, when the UIMs were removed, the low-affinity Ub binding patch on ENTH [18] interacted with the conjugated Ub on the Rsp5 ligase, and promoted its ubiquitylation on K103 or K148, as illustrated in Supplementary Figure S2. Our structural model suggests that K103 is facing the C-terminus of Ub. K148 is highly accessible for ubiquitylation, as the terminal helix of the short construct must move to accommodate the interaction with Ub, as seen in VHS domains [30,31].

### 3.3. Structure of Ent1–ENTH Provides Insight into Plasma Membrane Binding

The structure of a rat epsin–ENTH domain in a complex with PIP<sub>2</sub> (PDB accession code 1H0A) provided molecular insight into the mechanism of the lipid head recognition and membrane curvature [9]. In that study, McMahon and co-workers demonstrated that the binding of PIP<sub>2</sub> to the unstructured 17 residues at the N-terminus of ENTH induces the formation of an amphipathic  $\alpha$ -helix (H<sub>0</sub>) [9]. The hydrophobic face of H<sub>0</sub> dissolves into the inner leaflet of the lipid bilayer and induces membrane curvature. H<sub>0</sub> plays a pivotal role at both the beginning and end of endocytosis [9,15]. Positive residues at the hydrophilic face of H<sub>0</sub> interact with the PIP<sub>2</sub> lipid head-group (Figure 3). We determined the crystal structure of the yeast Ent1–ENTH domain that lacks the H<sub>0</sub> [18,19]. Given the high homology between the yeast and the rat epsin proteins, we constructed a structural model for H<sub>0</sub> (purple helix in Figure 3b). The superposition of the yeast Ent1–ENTH domain with the rat ENTH:PIP<sub>2</sub> complex provided insight into the molecular model for the interaction of the yeast protein with PIP<sub>2</sub> (Figure 3c,d). Binding takes place by a dozen amino acids comprising K3, R7, and K10 on  $\alpha$ H<sub>0</sub>, and K14 in the proceeding loop; residues R24, the backbone atoms of T27 and S28, and residue N29 all form  $\alpha$ H<sub>2</sub>, together with R62 (at  $\alpha$ H<sub>3</sub>), D65, Y69 (at the proceeding loop), and H72 from  $\alpha$ H<sub>4</sub>.

The structural model also sheds light on the electrostatic interactions of ENTH with PIPs. We employed the continuum solvation method APBS (Adaptive Poisson–Boltzmann Solver) with the CHARMM force field to calculate the electro-potential surface of ENTH. A positive (blue) surface located at the PIP<sub>2</sub> binding pocket was clearly observed. This positive patch probably attracts the negatively-charged lipid head, and provides an additional layer of information to ensure the specificity of Ent1, in order for it to interact with the plasma membrane (Figure 3e).

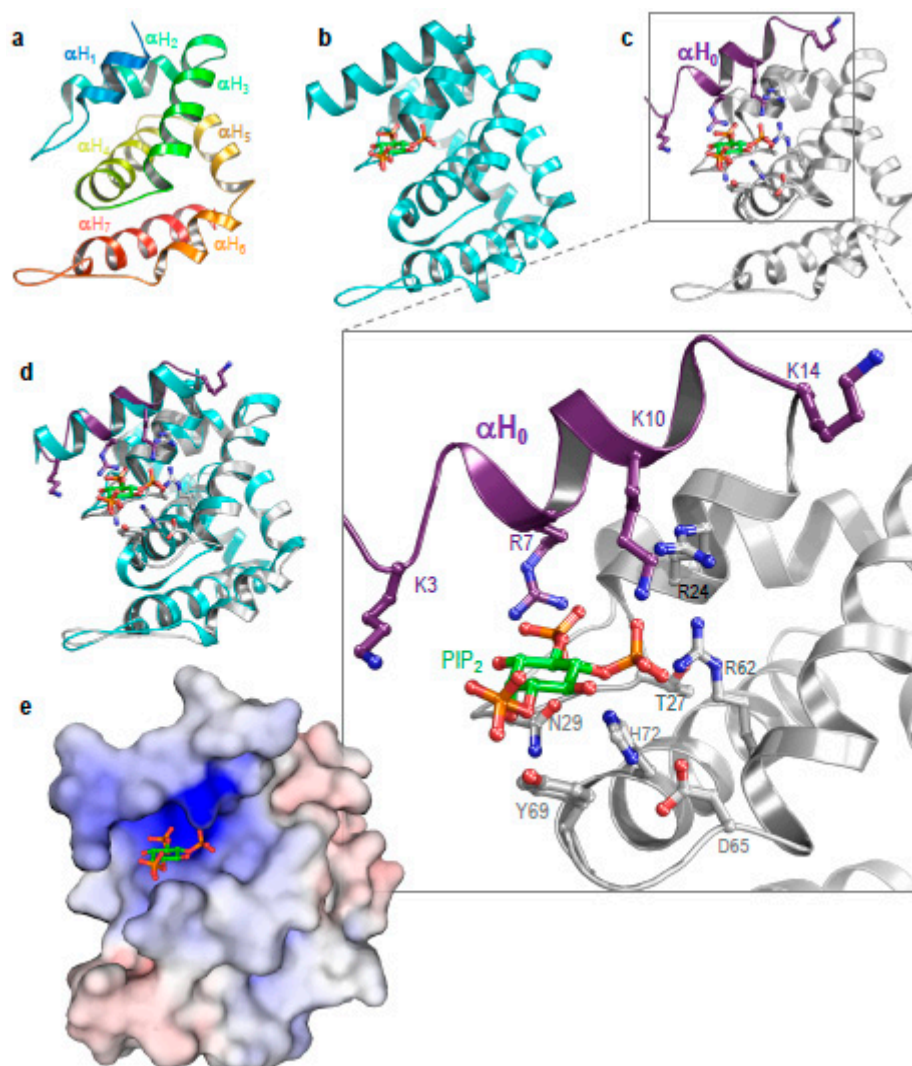


**Figure 3.** Structural insight into an ENTH domain. (a) The *apo* structure of Ent1-ENTH (PDB code 5LOZ). (b) The structure of a rat Epsin1-ENTH domain in complex with phosphatidylinositol-4,5-bisphosphate (PIP<sub>2</sub>; PDB code 1H0A). (c) A homology-based model of a yeast Ent1-ENTH domain with PIP<sub>2</sub>. Zooming in on the binding site shows the residues that interact with PIP<sub>2</sub> and K3. (d) The superposition of the yeast Ent1 model with rat Epsin1. (e) An electro-potential surface representation of the yeast Ent1-ENTH domain. PIP<sub>2</sub> is accommodated in a positively charged pocket (blue).

### 3.4. Ubiquitylation Regulates Epsin Membrane Binding In Vitro

Based on our finding that K3, a residue located at the edge of the PIP<sub>2</sub> binding site, undergoes ubiquitylation, we postulated that this modification would hinder PIP<sub>2</sub> binding and consequently dissociate Ent1 from the membrane. As ubiquitylation is a covalent modification, we predicted that it would exert a strong effect in the competition for the binding site. To test this hypothesis biochemically, we conducted two independent, *in vitro* competition experiments for the binding of *apo* Ent1 to PIP<sub>2</sub> versus ubiquitylated Ent1. Ent1 *apo* and ubiquitylated protein were purified as previously described [7,19]. First, we assessed the binding of the purified proteins to an immobilized PIP array (Figure 4). The PIP array membrane, which contains a concentration gradient of eight different phosphoinositides, was incubated with an equal quantity (1:1) mixture of *apo* Ent1<sub>1-184</sub> and ubiquitylated-Ent1<sub>1-184</sub>, and subjected to western blot analysis. To enable differential detection of the *apo* and the ubiquitylated-Ent1 proteins, an HA tag was fused to the C-terminus of the Ent1, and an His<sub>6</sub>-tag to the N-terminus of Ub. The results of the western analysis with anti-His<sub>6</sub> antibody were that ubiquitylated-Ent1 did not bind any of the PIPs in the array (Figure 4a). To verify that the lack

of signal was not due to the failure of the anti-His antibody to detect the His<sub>6</sub>-tag, we spotted the ubiquitylated-Ent1 sample on the same membrane (above the PI3P gradient), and repeated the western blot analysis with the same anti-His antibody. Indeed, clear western blot signals were found where the ubiquitylated-Ent1 was spotted (see spots in red oval dashed line at Figure 4b). The same PIP array membrane was then incubated with an anti-HA antibody. Western blot analysis with the anti-HA clearly showed specific binding to PI(3,4)P<sub>2</sub>, PI(4,5)P<sub>2</sub>, and PI(3,4,5)P<sub>3</sub>, for which the latter demonstrated an apparent higher affinity (Figure 4c). These results indicate that yeast Ent1 specifically binds several phosphatidylinositol moieties, and that Ent1 ubiquitylation negatively regulates this binding.

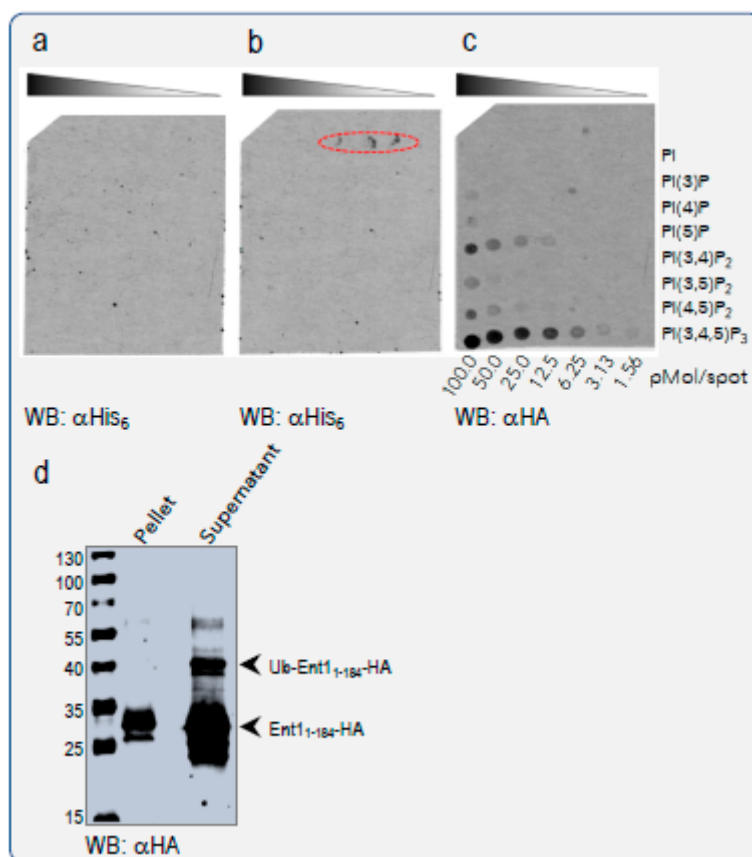


**Figure 4.** Ent1 and Ub-Ent1 PIPs binding assays in vitro. A 1:1 mix of purified *apo* and ubiquitylated Ent1<sub>1-184</sub> proteins was assayed for PIPs binding. A PIP array membrane (Echelon) was incubated with the protein mix and washed, as described in the Methods section. Proteins were detected by western blot (WB): *apo* with anti-His<sub>6</sub>-tag, and ubiquitylated Ent1 with anti-HA antibodies, respectively. (a) The PIP-array membrane after a binding assay with the mix and WB against the ubiquitylated Ent1. (b) The antibody reaction against ubiquitylated Ent1 that was blotted on the membrane, as described in the Results section. (c) The reaction with the HA antibody. The binding to the indicated PIPs is clearly seen as black spots. (d) A PI(4,5)P<sub>2</sub> enriched liposome (Echelon) binding assay. A protein mix contained *apo* and ubiquitylated Ent1<sub>1-184</sub> was used for a pull-down assay with PI(4,5)P<sub>2</sub> enriched liposomes. Following incubation, the liposomes were pelleted by centrifuge. Bound (Pellet) and unbound (Supernatant) proteins were then separated by SDS-PAGE, and detected by WB with anti-HA antibodies.

Interestingly, our binding assays revealed that the Ent1<sub>1-184</sub> presents a higher affinity to phosphatidylinositol(3,4,5)P<sub>3</sub> (PIP<sub>3</sub>). It is worth noting that, to the best of our knowledge, *S. cerevisiae* do not possess the pathway necessary for the synthesis of PIP<sub>3</sub>. Our structural model suggests that the Nζ atom of K3 is located at about 5 Å from the O3 atom of the inositol, a nearly ideal distance and

angle to accommodate and stabilize an additional phosphate group (not shown). In the ENTH:PIP<sub>2</sub> complex, however, K3 is accessible for ubiquitylation.

To further test the above hypothesis, in the second experiment we performed a liposome pelleting assay using PIP<sub>2</sub>-enriched membranes. One benefit of this *in vitro* assay is that it better mimics the natural membrane binding. PIP<sub>2</sub>-enriched liposomes were incubated with a mixture of *apo* and ubiquitylated Ent1<sub>1-184</sub> to enable binding. Bound and unbound proteins were then separated by sedimentation of the liposomes by ultra-centrifugation, as previously described by McMahon and co-workers [9]. Similar to the PIP-Array binding assay, we probed the pellet and the supernatant using an anti-HA antibody. We found a selective binding of only *apo* Ent1<sub>1-184</sub> to the PIP<sub>2</sub>-enriched liposomes (Figure 4d). Specifically, the *apo* protein was clearly visible in both bound and unbound fractions (pellet and supernatant, respectively). However, the ubiquitylated Ent1 was found only in the supernatant fraction, indicating that ubiquitylation had prevented the Ent1<sub>1-184</sub> from membrane binding.

### 3.5. Ubiquitylation Regulates the Plasma Membrane Association of Ent1 *In Vivo*

To test the hypothesis that the ubiquitylation of Ent1 regulates its membrane association *in vivo*, we sought to monitor the cellular localization of Ent1-GFP and constitutive ubiquitylated Ent1-GFP derivatives, using time-lapse fluorescent microscopy imaging in living cells. Deubiquitylases (DUBs) rapidly remove ubiquitylation signals, and therefore challenge such studies in eukaryotic cells. To circumvent this hurdle, we constructed a stable ubiquitylation mimicry fusion of Ent1-GFP. In these constructs, we mimicked ubiquitylation by fusing the carboxy terminus of Ub in-frame to the N-terminus of  $\Delta 3$ -Ent1-GFP (substituting K3; these constructs marked as Nter. Ub-fusion in Figure 5). Mimicking ubiquitylation by the fusion of Ub in-frame is sometimes valuable, especially when the authentic ubiquitylation site is located near one of the protein termini [32,33]. The high flexibility of the carboxy terminus tail of Ub probably compensates for the rigidity of the peptide bond between Ub and the N terminus of the target, compared to the iso-peptide bond formed with the ubiquitylated lysine residue. To eliminate the cleavage of Ub from the N-terminus by DUB(s) that cleave linear Ub chains, we substituted the terminal glycine with valine (Ub G76V) [34]. In the first *in vivo* experiment, we compared the localization of the full-length Ent1-GFP that was expressed from its natural genomic promoter [26,35] with that of the ectopic expression of  $\Delta 3$ -Ent1-GFP (Figure 5a,b, respectively). We found that both full-length and  $\Delta 3$ -Ent1 proteins are localized to the plasma membrane and to the cytosol. On the membrane, they seem to form clusters that probably represent endocytic puncta or early endosomes localization. Sometimes these proteins accumulate to the budding site, probably due to their function in recruitment of actin filament machinery (not shown).

Interestingly, the  $\Delta 3$ -Ent1 mutant presents a slightly more visibly stronger puncta adjacent to the plasma membrane (Figure 5b). This phenotype suggests that the elimination of K3 results in a less ubiquitylated phenotype, and consequently remains for a prolonged period on the early endosome membranes. Alternatively, it is certainly possible that the observed difference between the full-length and the  $\Delta 3$ -Ent1 mutant was also due to the difference in their expression levels. As stated earlier, the full-length protein is expressed from its normal chromosomal promoter, whereas the  $\Delta 3$ -Ent1 is expressed from a Gal promoter on a single-copy CEN (centromere) vector. Regardless of the origin of this difference, the bright phenotype of the ectopically-expressed  $\Delta 3$ -Ent1 is useful for assessing the possible regulation of ubiquitylation at K3 on Ent1 localization.

We next constructed several different Ent1/ENTH-GFP fusions and monitored their phenotypes (Figure 5c-j). We found that the ENTH<sub>4-152</sub> domain (Figure 5c) accumulated at the plasma membrane, but did not form puncta, unlike  $\Delta 3$ -Ent1 (Figure 5g,j), probably due to the lack of the C-terminal tail containing the Eps15 and clathrin-binding motifs. To examine the phenotype of Ent1 that is unable to directly associate with the plasma membrane, we deleted the entire H<sub>0</sub> helix by constructing ENTH<sub>18-152</sub>/Ent1<sub>18-454</sub>. Indeed, Figure 5d,h show that both  $\Delta H_0$ -ENTH and  $\Delta H_0$ -Ent1 proteins were localized only in the cytosol. These four variants provided clear visibility for membrane association versus cytosolic localization phenotypes, and therefore allowed us to assess the effect

of K3 ubiquitylation in vivo. We then monitored the phenotypes of Ub fusion at the N-termini of the ENTH domain and Ent1 proteins (Ub-ENTH<sub>4-152</sub>/Ub-Ent1<sub>4-454</sub>, namely Nter. Ub-fusion), which mimic the K3 ubiquitylated form. We found that both proteins localized only to the cytosol, identical to the  $\Delta H_0$  proteins (Figure 5e,i). This result suggests that K3 ubiquitylation hinders membrane association in vivo. We then sought to determine whether the membrane-dissociated phenotype is due to specific K3 ubiquitylation, rather than ubiquitylation per se. We therefore monitored the localization of chimeras in which Ub was fused to the C-termini (ENTH<sub>4-152</sub>-Ub-GFP/Ent1<sub>4-454</sub>-Ub-GFP; marked as Cter. Ub-fusion in Figure 5). We found that both fusions demonstrated membrane association and cytosolic phenotypes nearly identical to the unfused proteins (Figure 5f,j). Interestingly, it seems that the fusion of Ub at the C-terminus of Ent1<sub>4-454</sub> did not significantly affect the recruitment of the endocytic machinery, as observed by the puncta phenotype. Taken together, the results of the in vitro and in vivo experiments indicate that ubiquitylation at K3 dissociates Ent1 from the membrane.

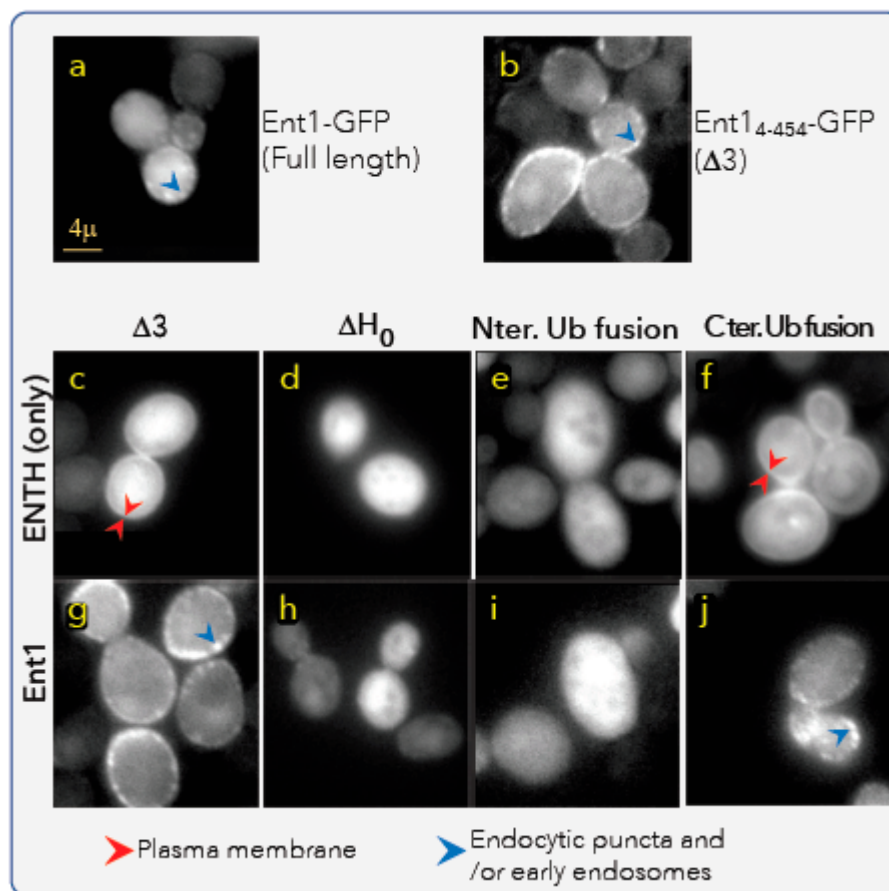


**Figure 5.** Ent1 and Ub–Ent1 membrane binding assays in vivo. Fluorescent microscopy imaging of living yeast cells expressing GFP fusion of the indicated Ent1 derivatives are shown. (a) A full-length Ent1 with C-terminus in-frame fusion GFP, expressed from the native genomic promoter. (b) An Ent1<sub>4-454</sub> ( $\Delta 3$ ) with C-terminus in-frame fusion GFP, expressed from a Gal promoter on a single copy plasmid. (c–j) The fluorescent readouts from indicated derivatives.  $\Delta H_0$  is the construct that lacks the first 17 residues. In the Ub-fusion constructs, Ub was fused in-frame instead of K3 (i.e., to residue Q4). In the fusion-Ub constructs, Ub is fused in-frame at the C-terminus of the Ent1 derivative (between Ent1 and GFP). Red arrows mark probably endocytic or early endosome clusters of Ent1–GFP; yellow arrows mark the accumulation of Ent1–GFP fusions at the plasma membrane.

#### 4. Discussion

Although the fate of ubiquitylation has been studied since the late 1970s, due to the extremely short life of ubiquitylated proteins, studies with purified ubiquitylated proteins are sparse. Our

*E. coli*-based expression system for the ubiquitylation cascade allowed us to purify milligram quantities of ubiquitylated proteins, which therefore played a pivotal role in this work [7].

Based on our current data, we propose the following model (Figure 6): membrane proteins (such as transporters, receptors, or channels) usually undergo ubiquitylation/clathrin-dependent endocytosis to terminate their function. Following ubiquitylation, the Ub receptor epsin reads and decodes the ubiquitylation signal into an endocytosis response by inducing membrane curvature and recruiting other endocytic proteins, such as Eps15 and clathrin. However, during the endocytosis process epsin is trafficked together with its cargo to early endosomes. To allow epsin to function again at the plasma membrane, a retrograde mechanism is needed. Our model suggests that Rsp5-dependent ubiquitylation of epsin takes place at the early endosome membrane on lysine residues at the periphery of the PIP<sub>2</sub> binding pocket. This ubiquitylation removes epsin from the membrane. We speculate that a deubiquitylation enzyme present in complex with Rsp5 then reverses the modification and allows epsin to bind the plasma membrane again.

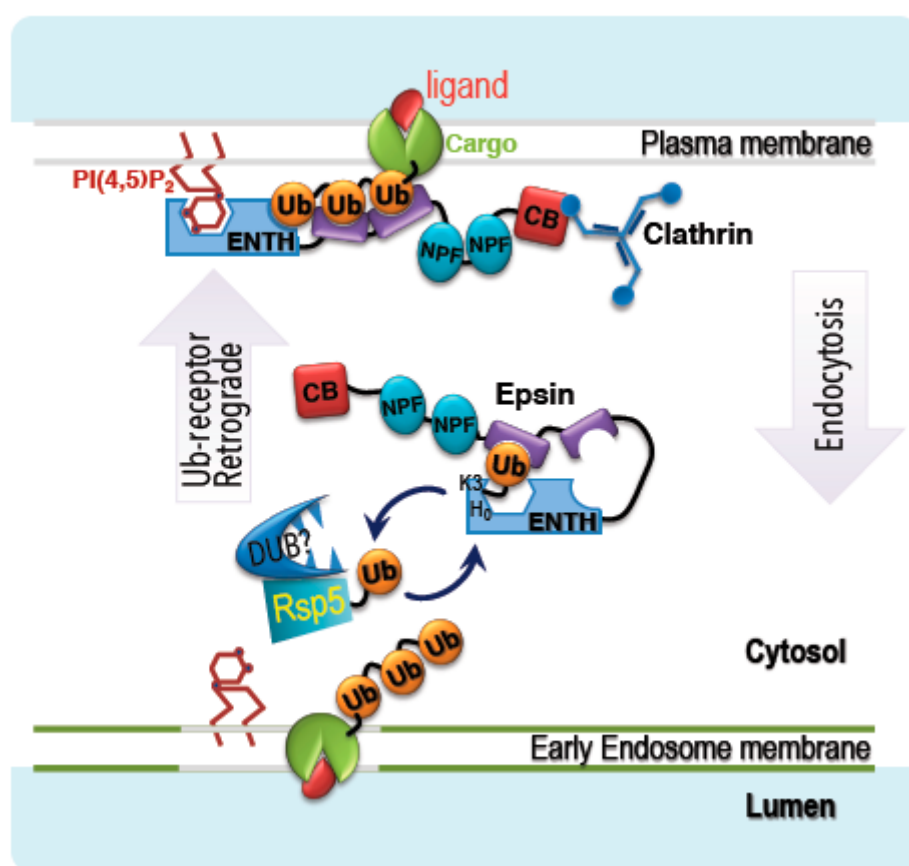


**Figure 6.** A model for the function of Ent1 ubiquitylation to initiate a retrograde process. Ent1 binds to the plasma membrane via the interaction of the ENTH domain with PIP<sub>2</sub>. The three UBDs of Ent1 bind to ubiquitylated cargo, and the clathrin binding box (CB) recruits clathrin proteins to promote endocytosis. For simplicity, other endocytic components (such as Eps15 that binds NPF modules) are not shown. Ent1 ubiquitylation takes place on early endosomes, probably by Rsp5, a process that dissociates Ent1 from the membrane. An uncharacterized deubiquitylase (DUB) that probably forms a complex with Rsp5 then removes Ub from ubiquitylated Ent1 to enable the cyclic function of Ent1.

Elegant recent structural studies by Meijers and co-workers on ENTH and ANTH domains (AP180 N-Terminal Homology) in complex with PIP<sub>2</sub> suggest that these domains form oligomers on the plasma membrane [36]. They show that unlike the rat Epsin1 (1H0A), the PIP<sub>2</sub> in the yeast Ent2 (5ON7) is sandwiched between two ENTH domains. Superposition of these structures revealed that the H<sub>0</sub> helices form a very different orientation with respect to the rest of the PIP<sub>2</sub> binding pockets.

While the entire structures are well imposed with RMSD values lower than 1 Å, comparing the axis of the H<sub>0</sub> helices show that they move by 53 and 59 degrees. Moreover, the PIP<sub>2</sub> molecules are not superimposed. They have opposite binding orientations, and are translated by about 5 Å from each other. Most importantly, regardless of these significant structural differences of H<sub>0</sub> structures, in both structures K3 is accessible for ubiquitylation (Supplementary Figure S3).

It will be interesting to explore the physiological function of K3 ubiquitylation. Wendland and co-workers demonstrated that the deletion of both redundant genes *ent1* and *ent2* is lethal, but could be complemented by the expression of the ENTH domain only [37]. The authors revealed a binding site on the ENTH for GAP proteins of Cdc42, needed for cell polarity. Our live imaging movies also show the accumulation of Ent1/ENTH at a patch in the plasma membrane, marking the budding site. This finding is in line with the ENTH function identified by Wendland. The redundancy and this additional function of Ent1/2 challenge the analyses of K3 ubiquitylation and deubiquitylation in endocytosis and budding.

Considering the existence of other membrane-associated proteins and ubiquitin receptors, and in light of the current findings, we suggest that ubiquitylation-dependent regulation is not restricted to epsin, but rather may exert a broader regulatory mechanism. Indeed, Yarden and co-workers have demonstrated that mono-ubiquitylation dissociates Lst2, a membrane-associated FYVE domain (Fab-1, YOTB, Vac-1, and EEA1) containing an adaptor, from early endosomes [38]. However, Lst2 ubiquitylation takes place far from the FYVE domain, demonstrating a diversification of mechanisms for the ubiquitylation-dependent regulation of membrane binding.

## 5. Conclusions

Like enzymes, Ub receptors function in a cyclic manner. They interact with their ubiquitylated substrates and decode the signal into a unique response in a spatiotemporal manner. The current study, together with several previous ones, has found that the ubiquitylation of Ub receptors functions to dissociate them from their products, and therefore promotes their cyclic activity. This cycle of ubiquitylation and deubiquitylation therefore positively regulates the Ub receptor activity. The typical prompt association and dissociation of UBDs from Ub moieties suggests that the Ub ligase and the DUB of Ub receptors may act within a complex to accelerate their function. Indeed, many ligases were found to form complexes with deubiquitylases.

Here, we demonstrated that epsin ubiquitylation blocks the context (membrane recognition) in order to dissociate the Ub-receptor from its new cellular context, and to retrograde the Ub-receptor to its original one. Considering previous studies that have demonstrated that ubiquitylation blocks the UBD [6–8]; we conclude that coupled mono-ubiquitylation [5,39] on one of the three main elements (UBD, context, and response) of Ub receptors functions to dissociate the receptor from its product. We therefore suggest that ubiquitylation and deubiquitylation modulate Ub receptors, and render them in an on/off manner to promote their cyclic activity.

**Supplementary Materials:** The Supplementary Materials are available online at <http://www.mdpi.com/2218-273X/9/8/325/s1>.

**Author Contributions:** N.T. constructed the clones, performed the biochemical and cellular experiments, and analyzed the data. O.K. designed and analyzed the mass spectrometry data. I.N. help to perform and analyze the live imaging experiments. G.P. conceived the hypothesis, designed the experiments, constructed the structural models, and wrote the paper.

**Funding:** This research was funded by grants from the Israel Science Foundation 464/11 and 651/16 to G.P., 1499/10 and 1665/16 to I.N., and 1623/17 and 2167/17 to O.K.

**Acknowledgments:** We thank Daniel Dar and Noa Reis for their dedicated and valuable help with the live imaging and the mass spectrometry experiments, respectively. We gratefully acknowledge Tal Keren-Kaplan, Ilan Attali, and Olga Levin-Kravets for technical assistance, for sharing clones and reagents, and for influential discussions.

**Conflicts of Interest:** The authors declare no conflict of interest.

## References

1. Weissman, A.M.; Shabek, N.; Ciechanover, A. The predator becomes the prey: Regulating the ubiquitin system by ubiquitylation and degradation. *Nat. Rev. Mol. Cell Biol.* **2011**, *12*, 605–620. [[CrossRef](#)]
2. Komander, D.; Rape, M. The ubiquitin code. *Annu. Rev. Biochem.* **2012**, *81*, 203–229. [[CrossRef](#)]
3. Hurley, J.H.; Lee, S.; Prag, G. Ubiquitin-binding domains. *Biochem. J.* **2006**, *399*, 361–372. [[CrossRef](#)]
4. Prag, G.; Misra, S.; Jones, E.A.; Ghirlando, R.; Davies, B.A.; Horazdovsky, B.F.; Hurley, J.H. Mechanism of ubiquitin recognition by the CUE domain of Vps9p. *Cell* **2003**, *113*, 609–620. [[CrossRef](#)]
5. Shih, S.C.; Prag, G.; Francis, S.A.; Sutanto, M.A.; Hurley, J.H.; Hicke, L. A ubiquitin-binding motif required for intramolecular monoubiquitylation, the CUE domain. *EMBO J.* **2003**, *22*, 1273–1281. [[CrossRef](#)]
6. Mattera, R.; Bonifacino, J.S. Ubiquitin binding and conjugation regulate the recruitment of Rabex-5 to early endosomes. *EMBO J.* **2008**, *27*, 2484–2494. [[CrossRef](#)]
7. Keren-Kaplan, T.; Attali, I.; Motamedchaboki, K.; Davis, B.A.; Tanner, N.; Reshef, Y.; Laudon, E.; Kolot, M.; Levin-Kravets, O.; Kleifeld, O.; et al. Synthetic biology approach to reconstituting the ubiquitylation cascade in bacteria. *EMBO J.* **2012**, *31*, 378–390. [[CrossRef](#)]
8. Keren-Kaplan, T.; Zeev Peters, L.; Levin-Kravets, O.; Attali, I.; Kleifeld, O.; Shohat, N.; Artzi, S.; Zucker, O.; Pilzer, I.; Reis, N.; et al. Structure of ubiquitylated-Rpn10 provides insight into its autoregulation mechanism. *Nat. Commun.* **2016**, *7*, 12960. [[CrossRef](#)]
9. Ford, M.G.; Mills, I.G.; Peter, B.J.; Vallis, Y.; Praefcke, G.J.; Evans, P.R.; McMahon, H.T. Curvature of clathrin-coated pits driven by epsin. *Nature* **2002**, *419*, 361–366. [[CrossRef](#)]
10. Shih, S.C.; Katzmann, D.J.; Schnell, J.D.; Sutanto, M.; Emr, S.D.; Hicke, L. Epsins and Vps27p/Hrs contain ubiquitin-binding domains that function in receptor endocytosis. *Nat. Cell Biol.* **2002**, *4*, 389–393. [[CrossRef](#)]
11. Aguilar, R.C.; Watson, H.A.; Wendland, B. The yeast Epsin Ent1 is recruited to membranes through multiple independent interactions. *J. Biol. Chem.* **2003**, *278*, 10737–10743. [[CrossRef](#)]
12. Wendland, B. Epsins: Adaptors in endocytosis? *Nat. Rev. Mol. Cell Biol.* **2002**, *3*, 971–977. [[CrossRef](#)]
13. Dupre, S.; Urban-Grimal, D.; Haguenaer-Tsapis, R. Ubiquitin and endocytic internalization in yeast and animal cells. *BBA Mol. Cell Res.* **2004**, *1695*, 89–111.
14. Campelo, F.; McMahon, H.T.; Kozlov, M.M. The hydrophobic insertion mechanism of membrane curvature generation by proteins. *Biophys. J.* **2008**, *95*, 2325–2339. [[CrossRef](#)]
15. Boucrot, E.; Pick, A.; Camdere, G.; Liska, N.; Evergren, E.; McMahon, H.T.; Kozlov, M.M. Membrane Fission Is Promoted by Insertion of Amphipathic Helices and Is Restricted by Crescent BAR Domains. *Cell* **2012**, *149*, 124–136. [[CrossRef](#)]
16. Ziv, I.; Matiuhin, Y.; Kirkpatrick, D.S.; Erpapazoglou, Z.; Leon, S.; Pantazopoulou, M.; Kim, W.; Gygi, S.P.; Haguenaer-Tsapis, R.; Reis, N.; et al. A perturbed ubiquitin landscape distinguishes between ubiquitin in trafficking and in proteolysis. *Mol. Cell. Proteom.* **2011**, *10*, M111-009753. [[CrossRef](#)]
17. Keller, A.; Eng, J.; Zhang, N.; Li, X.J.; Aebersold, R. A uniform proteomics MS/MS analysis platform utilizing open XML file formats. *Mol. Syst. Biol.* **2005**, *1*, 2005.0017. [[CrossRef](#)]
18. Levin-Kravets, O.; Tanner, N.; Shohat, N.; Attali, I.; Keren-Kaplan, T.; Shusterman, A.; Artzi, S.; Varvak, A.; Reshef, Y.; Shi, X.; et al. A bacterial genetic selection system for ubiquitylation cascade discovery. *Nat. Methods* **2016**, *13*, 945–952. [[CrossRef](#)]
19. Tanner, N.; Prag, G. Purification and crystallization of yeast Ent1 ENTH domain. *Acta Crystallogr. Sect. F Struct. Biol. Cryst. Commun.* **2012**, *68*, 820–823. [[CrossRef](#)]
20. Kelley, L.A.; Mezulis, S.; Yates, C.M.; Wass, M.N.; Sternberg, M.J.E. The Phyre2 web portal for protein modeling, prediction and analysis. *Nat. Protoc.* **2015**, *10*, 845–858. [[CrossRef](#)]
21. Emsley, P.; Cowtan, K. Coot: Model-building tools for molecular graphics. *Acta Crystallogr. Sect. D Biol. Crystallogr.* **2004**, *60*, 2126–2132. [[CrossRef](#)]
22. Murshudov, G.N.; Skubak, P.; Lebedev, A.A.; Pannu, N.S.; Steiner, R.A.; Nicholls, R.A.; Winn, M.D.; Long, F.; Vagin, A.A. REFMAC5 for the refinement of macromolecular crystal structures. *Acta Crystallogr. D* **2011**, *67*, 355–367. [[CrossRef](#)]
23. Schrodinger, LLC. *The PyMOL Molecular Graphics System, Version 1.8*; Schrodinger LLC: New York, NY, USA, 2015.
24. Jansen, G.; Wu, C.L.; Schade, B.; Thomas, D.Y.; Whiteway, M. Drag&Drop cloning in yeast. *Gene* **2005**, *344*, 43–51.

25. Swaney, D.L.; Beltrao, P.; Starita, L.; Guo, A.; Rush, J.; Fields, S.; Krogan, N.J.; Villen, J. Global analysis of phosphorylation and ubiquitylation cross-talk in protein degradation. *Nat. Methods* **2013**, *10*, 676–682. [[CrossRef](#)]
26. Huh, W.K.; Falvo, J.V.; Gerke, L.C.; Carroll, A.S.; Howson, R.W.; Weissman, J.S.; O’Shea, E.K. Global analysis of protein localization in budding yeast. *Nature* **2003**, *425*, 686–691. [[CrossRef](#)]
27. Lu, J.Y.; Lin, Y.Y.; Qian, J.; Tao, S.C.; Zhu, J.; Pickart, C.; Zhu, H. Functional dissection of a HECT ubiquitin E3 ligase. *Mol. Cell. Proteom.* **2008**, *7*, 35–45. [[CrossRef](#)]
28. Uchiki, T.; Kim, H.T.; Zhai, B.; Gygi, S.P.; Johnston, J.A.; O’bryan, J.P.; Goldberg, A.L. The ubiquitin-interacting motif protein, S5a, is ubiquitinated by all types of ubiquitin ligases by a mechanism different from typical substrate recognition. *J. Biol. Chem.* **2009**, *284*, 12622–12632. [[CrossRef](#)]
29. Isasa, M.; Katz, E.J.; Kim, W.; Yugo, V.; Gonzalez, S.; Kirkpatrick, D.S.; Thomson, T.M.; Finley, D.; Gygi, S.P.; Crosas, B. Monoubiquitination of RPN10 regulates substrate recruitment to the proteasome. *Mol. Cell* **2010**, *38*, 733–745. [[CrossRef](#)]
30. Ren, X.; Hurley, J.H. VHS domains of ESCRT-0 cooperate in high-avidity binding to polyubiquitinated cargo. *EMBO J.* **2010**, *29*, 1045–1054. [[CrossRef](#)]
31. Misra, S.; Beach, B.M.; Hurley, J.H. Structure of the VHS domain of human Tom1 (target of myb 1): Insights into interactions with proteins and membranes. *Biochemistry* **2000**, *39*, 11282–11290. [[CrossRef](#)]
32. Joshi, A.; Munshi, U.; Ablan, S.D.; Nagashima, K.; Freed, E.O. Functional replacement of a retroviral late domain by ubiquitin fusion. *Traffic* **2008**, *9*, 1972–1983. [[CrossRef](#)] [[PubMed](#)]
33. Donaldson, K.M.; Yin, H.; Gekakis, N.; Supek, F.; Joazeiro, C.A. Ubiquitin signals protein trafficking via interaction with a novel ubiquitin binding domain in the membrane fusion regulator, Vps9p. *Curr. Biol.* **2003**, *13*, 258–262. [[CrossRef](#)]
34. Lindsten, K.; Menendez-Benito, V.; Masucci, M.G.; Dantuma, N.P. A transgenic mouse model of the ubiquitin/proteasome system. *Nat. Biotechnol.* **2003**, *21*, 897–902. [[CrossRef](#)] [[PubMed](#)]
35. Ghaemmaghami, S.; Huh, W.K.; Bower, K.; Howson, R.W.; Belle, A.; Dephoure, N.; O’Shea, E.K.; Weissman, J.S. Global analysis of protein expression in yeast. *Nature* **2003**, *425*, 737–741. [[CrossRef](#)] [[PubMed](#)]
36. Garcia-Alai, M.M.; Heidemann, J.; Skruzny, M.; Gieras, A.; Mertens, H.D.T.; Svergun, D.I.; Kaksonen, M.; Uetrecht, C.; Meijers, R. Epsin and Sla2 form assemblies through phospholipid interfaces. *Nat. Commun.* **2018**, *9*, 328. [[CrossRef](#)] [[PubMed](#)]
37. Aguilar, R.C.; Longhi, S.A.; Shaw, J.D.; Yeh, L.Y.; Kim, S.; Schon, A.; Freire, E.; Hsu, A.; McCormick, W.K.; Watson, H.A.; et al. Epsin N-terminal homology domains perform an essential function regulating Cdc42 through binding Cdc42 GTPase-activating proteins. *Proc. Natl. Acad. Sci. USA* **2006**, *103*, 4116–4121. [[CrossRef](#)] [[PubMed](#)]
38. Mosesson, Y.; Chetrit, D.; Schley, L.; Berghoff, J.; Ziv, T.; Carvalho, S.; Milanezi, F.; Admon, A.; Schmitt, F.; Ehrlich, M.; et al. Monoubiquitylation regulates endosomal localization of Lst2, a negative regulator of EGF receptor signaling. *Dev. Cell* **2009**, *16*, 687–698. [[CrossRef](#)]
39. Woelk, T.; Oldrini, B.; Maspero, E.; Confalonieri, S.; Cavallaro, E.; Di Fiore, P.P.; Polo, S. Molecular mechanisms of coupled monoubiquitination. *Nat. Cell Biol.* **2006**, *8*, 1246–1254. [[CrossRef](#)]

